ACS AUTHORCHOICE Letter

NANO LETTERS

Cite This: Nano Lett. 2020, 20, 652−657

pubs.acs.org/NanoLett

Sequential Bending and Twisting around C−C Single Bonds by Mechanical Lifting of a Pre-Adsorbed Polymer

Rémy Pawlak,*[,†,▽] J. G. Vilhena,*[,†,▽] Philipp D'Astolfo,[†] Xunshan Liu,[‡] Giacomo Prampolini,[§] Tobias Meier,[†] Thilo Glatzel,[†] Justin A. Lemkul,[∥] Robert Häner,[‡] Silvio Decurtins,[‡] Alexis Baratoff,[†] Rubén Pérez,[⊥,#] Shi-Xia Liu,[‡] and Ernst Meyer*[,†]

[†]Department of Physics, University of Basel, Klingelbergstrasse 82, 4056 Basel, Switzerland

[‡]Department of Chemistry and Biochemistry, University of Bern, Freiestrasse 3, Bern, CH 3012, Switzerland

[§]CNR−Consiglio Nazionale delle Ricerche, Istituto di Chimica dei Composti Organo Metallici (ICCOM-CNR), Pisa, Italy

[∥]Department of Biochemistry, Virginia Tech, 303 Engel Hall, 340 West Campus Drive, Blacksburg, Virginia 24061, United States

[⊥]Departamento de Física Teórica de la Materia Condensada, Universidad Autónoma de Madrid, E-28049 Madrid, Spain

[#]Condensed Matter Physics Center (IFIMAC), Universidad Autónoma de Madrid, E-28049 Madrid, Spain

Supporting Information

ABSTRACT: Bending and twisting around carbon−carbon single bonds are ubiquitous in natural and synthetic polymers. Force-induced changes were so far not measured at the single-monomer level, owing to limited ways to apply local forces. We quantified down to the submolecular level the mechanical response within individual poly-pyrenylene chains upon their detachment from a gold surface with an atomic force microscope at 5 K. Computer simulations based on a dedicated force field reproduce the experimental traces and reveal symmetry-broken bent and rotated conformations of the sliding physisorbed segment besides steric hindrance of the just lifted monomer. Our study also shows that the tip−molecule bond remains intact but remarkably soft and links force variations to complex but well-defined conformational changes.

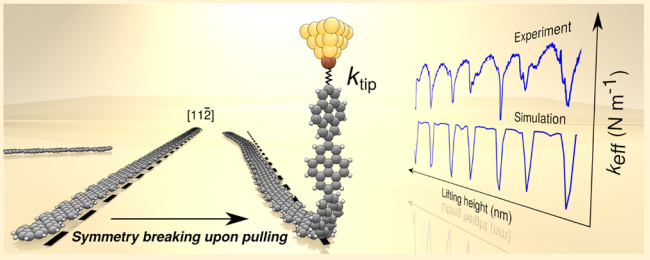

KEYWORDS: *Atomic force microscopy (AFM), force spectroscopy, molecular dynamics (MD) simulations, pyrenylene chains, nanoscale friction, mechanics*

Rotation around a carbon−carbon single bond is at the basis of conformational isomerism, catalytic reactions, and photochromism. Such local changes can be activated by heating, irradiation, or electrical potential which overcome potential energy barriers, whereas mechanical force is considered as invasive, i.e., capable of rupturing covalent bonds in polymers.[1,2] As recognized in rotaxanes[3] and catenanes,[4] intramolecular stress from repulsions of non-bonded atoms causes variations of bond lengths, angles, and torsions of the molecular structure. This mechanical response is relevant for the design, synthesis, and operation of molecular switches or motors, capable of converting external stimuli into specific movements.[5,6] To date, it has been challenging to apply and assess the effect of a local force within a single molecule, since its dynamical behavior is usually affected by thermal fluctuations.[7−9]

An elegant way to establish a connection between local single-molecule deformations and an external force is the use of a low-temperature atomic force microscope (AFM) operated in an ultrahigh vacuum.[10] Polycyclic aromatic hydrocarbons (PAHs), such as graphene nanoribbons (GNRs), can be synthesized in situ from evaporated precursors on atomically clean surfaces.[11] The formed structures are directly characterized on the atomic scale by combined scanning tunneling microscopy (STM) and dynamic AFM.[12] In addition, tip-assisted manipulation experiments can control their displacements.[13−15]

With the advent of cryo-force spectroscopy,[16−18] the detection of a molecule mechanical response is now possible down to the submolecular level under tensions of a few tens of pico-Newtons up to nano-Newtons. The selected end of a single molecule or polymer chain is contacted by the tip apex and pulled vertically from a surface.[19−22] The recorded signal reflects complex dynamical phenomena between the tip and the sample, e.g., the adhesion and succesive detachment of subunits, as well as the dynamics of the segment still sliding over the surface. An in-depth theoretical understanding of the dynamic behavior of detaching and sliding contacts as an

Received: October 25, 2019
Revised: December 2, 2019
Published: December 4, 2019

DOI: 10.1021/acs.nanolett.9b04418
Nano Lett. 2020, 20, 652−657

ensemble requires careful modeling and extensive numerical simulations.[17,18,20,23−26]

To benchmark the detection of molecular deformations and motions, we investigated a long poly(2,7-pyrenylene) chain adsorbed on Au(111) and its lifting response using cryo-force spectroscopy. While pyrene[27] stands as a paradigm PAH and for the synthesis of long functional polymers,[28] we extended its synthesis to surfaces using Ullman reaction of 2,7-di-bromo-pyrene precursors (Figure 1a and Supporting Figure S1). Our

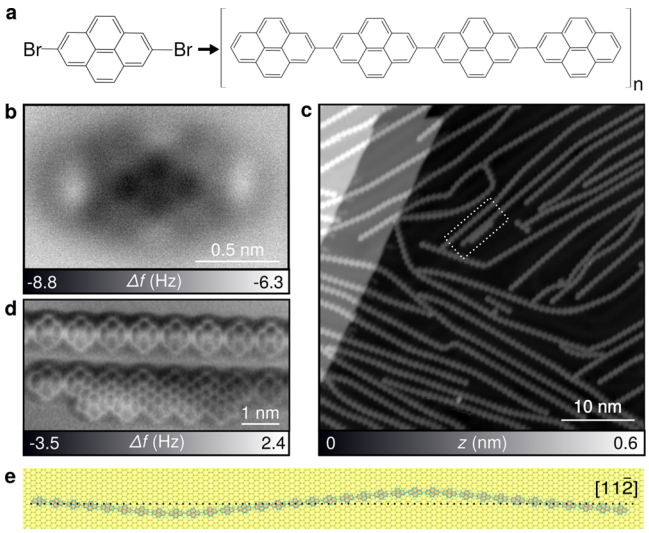

Figure 1. Poly(2,7-pyrenylene) chain adsorption on Au(111). (a) Ullmann reaction of the 2,7-dibromopyrene precursor on Au(111). (b) AFM image of the unreacted precursor using a CO-functionalized tip. (c) STM overview of the reacted chains on Au(111) (I_t = 1 pA, V_{tip} = −0.35 mV). (d) Close-up AFM image of the single and fused double poly(2,7-pyrenylene) chains within the dotted rectangle in part c (oscillation amplitude: A = 50 pm, V_{tip} = 0 V). (e) Equilibrium configuration obtained from MD simulations of the 35-unit poly(2,7-pyrenylene) chain initially adsorbed straight along the [11$\bar{2}$] Au(111) direction.

measurements also complement recent studies using polymeric chains and ribbons that revealed voltage-dependent conductance,[19] the detection of GNR bright luminescence,[22] or superlubric sliding behavior.[17,25,29] While GNRs are more rigid transverse to their growth direction, our system involves C−C single bonds between monomers which lower in-plane and out-of-plane chain stiffness. In contrast to dimethyl substituted polyfluorene,[16,19,24] unreacted precursors and polymerized chains (Figure 1b and d) adsorb flat along face cubic centered (fcc) valleys of the Au(111) reconstruction. AFM measurements with CO-terminated tips[12] confirmed single C−C bonds between monomers (Figure 1d). Long poly(2,7-pyrenylene) chains are aligned along the [11$\bar{2}$] and equivalent directions but show in-plane bending (Figure 1c) that can be easily modified by tip manipulations (Supporting Figure 2).

To rationalize the chain conformations, we employed a multilevel computational approach[30] combining quantum mechanical (QM) and molecular dynamics (MD) simulations (see Methods and Supporting Figures S3 and S4). The computed length between adsorbed units is 0.86 nm compared to the experimental AFM value (0.84 nm). Simulated temperature quenching of a 35-unit chain initially aligned straight along the [11$\bar{2}$] direction (Supporting Movie S1) shows strong in-plane bending fluctuations which gradually lead to bent final geometries (Figure 1e and Supporting Figure S6). These deformations originate from bond angle variations between adsorbed units favoring the polymer−surface registry (see Supporting Information S3). A variety of adsorbed chain configurations is obtained in both simulations and experiments (Supporting Figure S6), in agreement with polyfluorene chains on Au(111)[16] but in stark contrast to armchair GNRs adsorbed straight along [10$\bar{1}$] equivalent directions.[17]

A representative experimental trace of the effective system stiffness $k_{eff}(Z)$ versus lifting height Z (see the Methods) is shown in Figure 2b for a chain of n = 35 pyrenylene units, as determined by STM (Figure 2a). The detected signal exhibits dips (dashed lines) attributed to single monomer detachments.[16] For $Z \leq 1.5$ nm, k_{eff} dips below 1 N m^{-1} and then rises, due to superimposed electrostatic and van der Waals tip−sample interactions. The assignment of the first two detachments is difficult until the signal becomes regular for $Z \geq 1.5$ nm, with maxima of 0.2 N m^{-1} consistent with a remarkably soft but intact tip−chain bond and a high stretch stiffness of the chain which also favors nearly frictionless sliding on the surface.[16,17,25] The lifting is completed when Z = 27.9 nm, corresponding to an average detachment spacing of $L = Z_{off}/33$ = 0.84 nm per unit, counting the detachments from n = 2. Figure 2c shows the smoothed computed $k_{eff}(Z)$ of a 35-unit chain lifted from an unreconstructed Au(111) surface using steered MD simulations (see Methods).[18] The bond between the tip and the molecule is modeled via a harmonic spring of stiffness k_{tip} connecting the first pyrenylene unit para-carbon atom, whose motion is frozen along the X and Y directions, to a virtual atom moved at constant velocity along Z (further details are provided in the Methods). The trace reproduces the detachment of n = 33 monomers attained for a relative lifting height of Z_{off} = 28.6 nm, corresponding to L = 0.87 nm, in agreement with experimental (0.84 nm) and computed (0.86 nm) values. Supporting Movies S2 and S3 confirm the assignment of the dips to successive monomer detachments.

A closer inspection reveals two alternating detachment spacings. As illustrated in Figure 3a for $7 \leq n \leq 13$, long $L^+ \approx$ 920 pm and short $L^- \approx$ 770 pm values alternate. Parts B, C, and D of Figure 3 display the computed normal force $F(Z)$, the stiffness $k_{eff}(Z) = dF/dZ$, and the twist angle ϕ between the planes of consecutive pyrenylene units. The twist angles of the lifted even (green) and odd (purple) units (ϕ_{n-1} = −20 or +30° in Figure 3d) relative to still adsorbed units n do not appear very different in the top views (Figure 3e vs Figure 3f). Indeed, the −8° twist of even units prior to detachment is expected to combine with −20° afterward. Actually (see Supporting Information S4), both lifted units are rotated by ±30° with respect to their axes inclined by about 30° with respect to the surface normal. As lifting proceeds, ϕ approaches the equilibrium gas-phase values $\phi_{eq} = \pm 40°$ (Supporting Figures S4 and S5) along the lifted segment which then becomes straight and inclined by at most 10°. The inclinations and incomplete twists of the just lifted units reflect the competition between the energy gain from twisting (Supporting Figure S4) and the remaining attraction to the surface which causes steric hindrance (Supporting Table S1).

$F(Z)$ exhibits ramps of nearly constant slope separated by drops, consistent with the appearance of $k_{eff}(Z)$. The force maxima at the end of L^+ ramps (0.40 nN on average) are higher compared to L^- ramps (0.38 nN on average). The corresponding work increments on the pulled chain (areas under the respective "sawteeth"), 180 and 146 kJ mol^{-1},

DOI: 10.1021/acs.nanolett.9b04418
Nano Lett. 2020, 20, 652−657

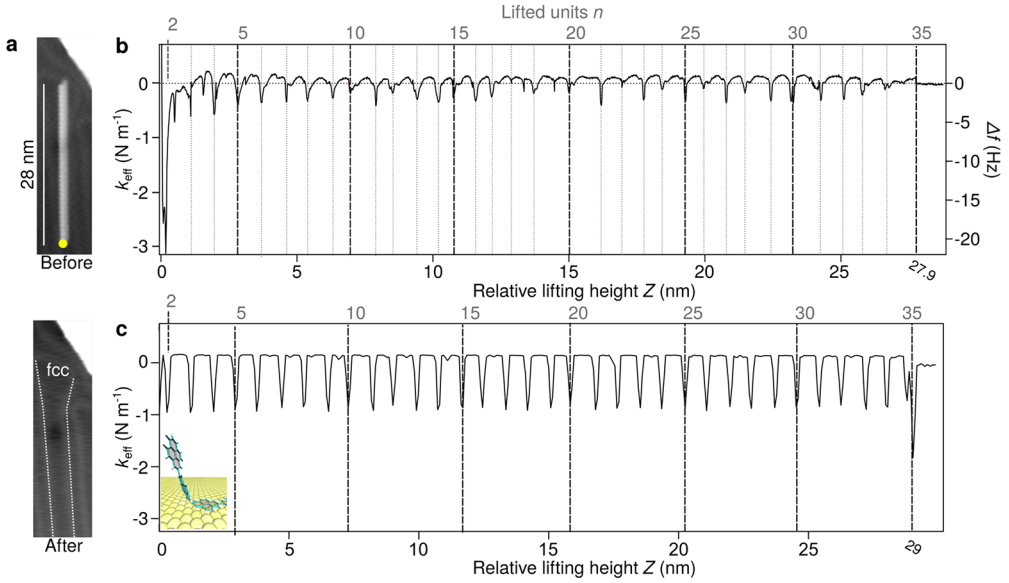

Figure 2. Mechanical response of a poly(2,7-pyrenylene) chain during lifting. (a) STM images of a chain before and after the lifting experiment (I = 1 pA, V_{tip} = −150 mV). (b) Experimental retraction trace k_{eff} as a function of the lifting height Z with respect to the pickup point. The top axis labels dips associated with single monomer detachments and marked by dashed lines with an average separation of $L \approx 0.84$ nm. (c) Computed $k_{eff}(Z)$ shifted such that the n = 2 dips coincide; units are completely detached at Z = 28.6 nm, which corresponds to $L \approx 0.87$ nm.

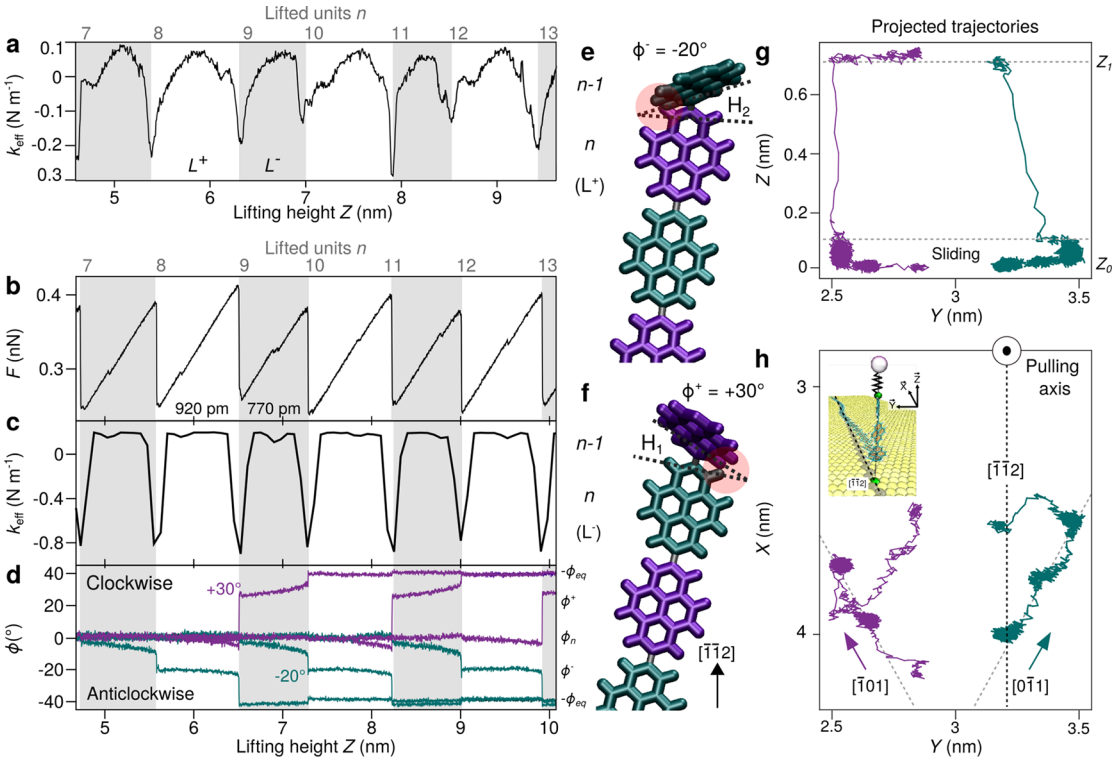

Figure 3. Assignment of detachment spacings and mechanical twists. (a) Experimental $k_{eff}(Z)$ traces for $7 \le n \le 13$ detachments revealing alternating spacings L^- = 0.77 nm (gray) and L^+ = 0.92 nm (white). (b) Computed normal force $F(Z)$, (c) associated stiffness $k_{eff}(Z)$, and (d) angle $\phi(Z)$ between consecutive monomer planes. (e and f) MD snapshots prior to clockwise and anticlockwise twists of odd and even units n sterically hindered (red circles) by lifted units $n-1$. (g and h) Projected trajectories of hydrogen atoms H_2 (n = 9, purple) and H_1 (n = 10, green) before and after their detachments. Before detaching, the units slide along equivalent Au(111) directions with different offsets relative to the pulling axis, leading to higher F maxima and hence longer L^+ for odd n.

respectively, exceed by far the 8 kJ mol^{-1} maximum energy gain from twisting each lifted unit (Supporting Figure S4) but are comparable to the desorption energy per unit, e.g., $(E_{chain} - E_{ads})/35$ = 137 kJ mol^{-1} in the starting configuration of Supporting Figure S6b according to Supporting Table S1. The L^-, L^+ alternation arises from differences in the energy cost of lifting odd vs even units which include the cost of bending C−C bonds between units. This energy is mainly localized between units n and $n-1$, in analogy to mechanically interlocked parts of molecular machines.[4,5] As seen in Figure

DOI: 10.1021/acs.nanolett.9b04418
Nano Lett. 2020, 20, 652−657

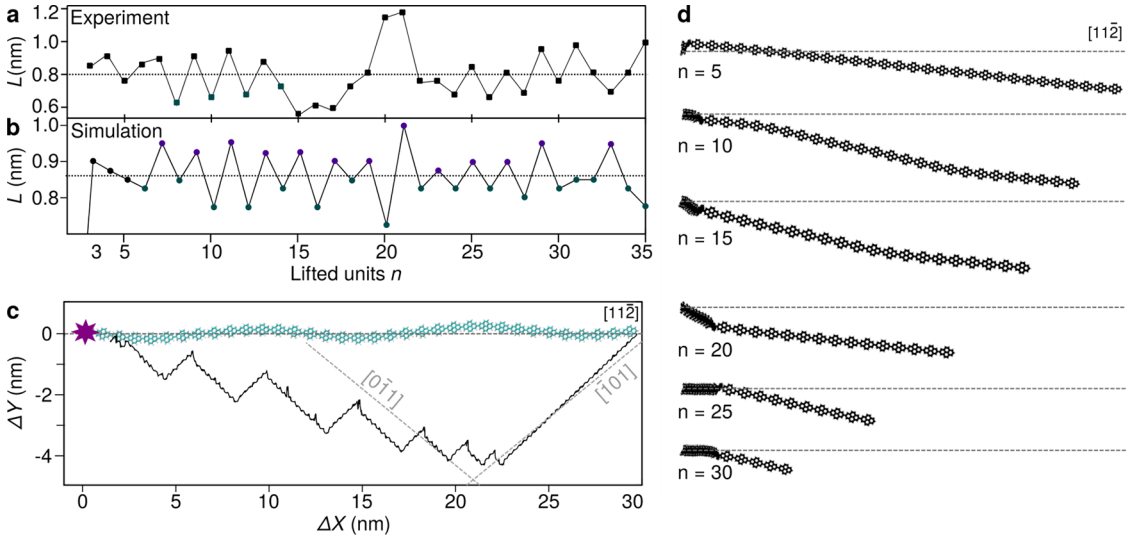

Figure 4. Nontrivial surface dynamics of the 35-unit chain during lifting. (a and b) Experimental and computed detachment spacing versus n. (c) Surface displacement of the tail C atom. For $n \leq 6$, the chain spontaneously breaks its initial symmetric configuration. Monomers slide alternatively along nominally equivalent [$\bar{1}$00] and [$\bar{1}$01] Au(111) directions toward the lifting axis (purple star) about a rotated mean direction. (d) Snapshots of the chain conformation for selected n values. The crowded symbols identify the slightly inclined lifted segment and the shifting detachment points.

3g and h as well as Supporting Movies S2 and S3, odd (n = 9) and even (n = 10) units behave differently (see Supporting Figures S7 and S8 and Supporting Information S7). Before detaching, they move approximately along the [$\bar{1}$01] and [0$\bar{1}$1] directions of least corrugation along the Au(111) surface, away from and toward the initial chain alignment axis, respectively. This asymmetric motion induces lateral forces which modulate the inclination of the n to n − 1 C−C bond. The normal component of the tension sensed by the tip is only slightly affected because the lifted segment becomes almost vertical after the first unit is lifted (in contrast to fused armchair GNRs which bend gradually[17,25]). The different force maxima and the L^-, L^+ alternation are most likely caused by asymmetric C−C bond bending. The stick−slip motion of the sliding chain segment induces some friction, besides small dips atop $k_{eff}(Z)$ maxima[16] which are better resolved in parallel pulling studies.[17]

Parts a and b of Figure 4 show that the alternation also appears for 22 ≤ n ≤ 30, besides irregularities near the ends and the center of the pulling range. Supporting Movie S2 illustrates the underlying configurational changes. The sliding segment develops a symmetry-broken rotated configuration, while the first six units are lifted and the tail unit executes stick−slip motion in the [$\bar{1}$01] direction (Figure 4c). Later, the motion switches between the two favored sliding directions, also for other units. Together with transverse shifts of the detachment point seen in Figure 4d, this induces fluctuations in the mean orientation and in-plane bending of the sliding segment as it adjusts to optimize its surface registry. Finally, Supporting Movie S4 and Supporting Figure S9 show that the rotation is triggered once the first unit is lifted, in the same sense as it is twisted, e.g., downward if the twist is clockwise.

Assisted by dedicated numerical simulations, cryo-force spectroscopy can recognize subtle conformational changes of a pulled polymer at the single-bond level, thus opening new avenues for the design of molecular components able to convert mechanical energy into predefined motion.

■ ASSOCIATED CONTENT

Supporting Information

The Supporting Information is available free of charge at https://pubs.acs.org/doi/10.1021/acs.nanolett.9b04418.

Methods; Supporting Information S1−S5; Figure S1, polymerization of single 2,7-pyrenylene precursors; Figure S2, tip-induced lateral manipulation of single poly(2,7-pyrenylene) chains; Figure S3, Joyce force field labels and internal coordinates; Figure S4, comparison between QM and fitted classical FF vibrational modes and torsion potential of the 2,7-pyrenylene trimer; Figure S5, gas-phase configurations of the poly(2,7-pyrenylene) chain; Figure S6, relaxed configurations of poly(2,7-pyrenylene) adsorbed on Au(111); Figure S7, different motions of even versus odd detaching units; Figure S8, different motions of front versus tail hydrogen atoms; Figure S9, correlation between adsorbed chain dynamics and twist of lifted units; Table S1, JOYCE FF energy components for the different adsorption configurations in Supporting Figure S6 (PDF)

Supplementary Movie 1: MD quenching simulation of the pre-adsorbed poly(2,7-pyrenylene). The initial conguration is shown in Supporting Figure S6a and the nal conguration of Figure 1e. The quenching proceeds from 350 K to 5 K with a cooling rate of 0.0345 K ps^{-1} (MPG)

Supplementary Movie 2: Top view of the lifting simulation starting from the conguration in Supporting Figure S6b (pink underlying Au atoms) illustrating many a priori unexpected conguration changes of the still adsorbed chain segment which occur as successive monomers twist as they are lifted. For clarity purpose, only the just detached units are shown in the movie (MPG)

Supplementary Movie 3: Side view of the same lifting simulation illustrating the alternating twists of the lifted units and the nearly vertical inclination of the lifted chain segment which slightly changes as the following

DOI: 10.1021/acs.nanolett.9b04418
Nano Lett. 2020, 20, 652−657

adsorbed units slide towards the lifting axis. Side view of the lifting simulation of Supplementary Movies 2-3, showing the pulled atom moving at constant XY while the angle between the lifted segment and the pulling axis remain small after the rst two units detach (MPG)

Supplementary Movie 4: Inuence of the in-plane bending induced at the start of pulling on the twist of the rst lifted unit and the subsequent symmetry-breaking. The chain highlighted in black is the same as in Supplementary Movie S2 and S3, whereas the chain highlighted in purple exhibits an initial curvature and subsequent changes that mirror the behavior of the chain represented in black. This initial dierence of stochastic origin gives rise to a downward/upward rotation of the chain tail (MPG)

AUTHOR INFORMATION

Corresponding Authors

*E-mail: remy.pawlak@unibas.ch.
*E-mail: guilhermevilhena@gmail.com
*E-mail: ernst.meyer@unibas.ch.

ORCID

Rémy Pawlak: 0000-0001-8295-7241
J. G. Vilhena: 0000-0001-8338-9119
Giacomo Prampolini: 0000-0002-0547-8893
Tobias Meier: 0000-0003-0606-5131
Thilo Glatzel: 0000-0002-3533-4217
Justin A. Lemkul: 0000-0001-6661-8653
Robert Häner: 0000-0001-5014-4318
Rubén Pérez: 0000-0001-5896-541X
Ernst Meyer: 0000-0001-6385-3412

Author Contributions

[▽]R.P., J.G.V.: These authors equally contributed.

Author Contributions

E.M., R.P., S.D., and S-X.L. conceived the experiments. S.D., S.-X.L., and X.L. synthesized the polymer precursors. R.P. and P.D. performed the STM/AFM measurements and lifting experiments. J.G.V. conducted the numerical simulations. R.P. and J.G.V. analyzed the data with A.B., R.P., and G.P. R.P., J.G.V., A.B. and P.D. wrote the manuscript. All authors discussed the results and revised the manuscript.

Notes

The authors declare no competing financial interest.

ACKNOWLEDGMENTS

A.B., E.M., R.P., T.G., and T.M. thank the Swiss National Science Foundation (SNF), the Swiss Nanoscience Institute (SNI), and the European Research Council (ERC) under the European Union's Horizon 2020 research and innovation program (Grant Agreement No. 834402). The COST Action MP1303 is gratefully acknowledged. J.G.V. and R.P. acknowledge the Spanish MINECO (projects MDM-2014-0377, MAT2014-54484-P, and MAT2017-83273-R) and the assistance and computing resources from Red Española de Supercomputación (RES-BSC) and ICCOM-PI (CNR) HPC computational facilities. J.G.V. acknowledges funding from a Marie Sklodowska-Curie Fellowship within the Horizons 2020 framework (DLV-795286).

REFERENCES

(1) Beyer, M. K.; Clausen-Schaumann, H. Mechanochemistry: The Mechanical Activation of Covalent Bonds. *Chem. Rev.* **2005**, *105*, 2921−2948.
(2) Hickenboth, C. R.; Moore, J. S.; White, S. R.; Sottos, N. R.; Baudry, J.; Wilson, S. R. Biasing Reaction Pathways With Mechanical Force. *Nature* **2007**, *446*, 423.
(3) Balzani, V.; Credi, A.; Raymo, F. M.; Stoddart, J. F. Artificial Molecular Machines. *Angew. Chem., Int. Ed.* **2000**, *39*, 3348−3391.
(4) Wasserman, E. The Preparation of Interlocking Rings: A Catenane. *J. Am. Chem. Soc.* **1960**, *82*, 4433−4434.
(5) Stoddart, J. F. The Chemistry of The Mechanical Bond. *Chem. Soc. Rev.* **2009**, *38*, 1802−1820.
(6) Roke, D.; Wezenberg, S. J.; Feringa, B. L. Molecular rotary motors: Unidirectional motion around double bonds. *Proc. Natl. Acad. Sci. U. S. A.* **2018**, *115*, 9423−9431.
(7) Brough, B.; Northrop, B. H.; Schmidt, J. J.; Tseng, H.-R.; Houk, K. N.; Stoddart, J. F.; Ho, C.-M. Evaluation of synthetic linear motor-molecule actuation energetics. *Proc. Natl. Acad. Sci. U. S. A.* **2006**, *103*, 8583−8588.
(8) Janke, M.; Rudzevich, Y.; Molokanova, O.; Metzroth, T.; Mey, I.; Diezemann, G.; Marszalek, P. E.; Gauss, J.; Böhmer, V.; Janshoff, A. Mechanically interlocked calix[4]arene dimers display reversible bond breakage under force. *Nat. Nanotechnol.* **2009**, *4*, 225.
(9) Sluysmans, D.; Hubert, S.; Bruns, C. J.; Zhu, Z.; Stoddart, J. F.; Duwez, A.-S. Synthetic oligorotaxanes exert high forces when folding under mechanical load. *Nat. Nanotechnol.* **2018**, *13*, 209−213.
(10) Giessibl, F. J. The qPlus sensor, a powerful core for the atomic force microscope. *Rev. Sci. Instrum.* **2019**, *90*, No. 011101.
(11) Cai, J.; Ruffieux, P.; Jaafar, R.; Bieri, M.; Braun, T.; Blankenburg, S.; Muoth, M.; Seitsonen, A. P.; Saleh, M.; Feng, X.; Müllen, K.; Fasel, R. Atomically precise bottomup fabrication of graphene nanoribbons. *Nature* **2010**, *466*, 470.
(12) Gross, L.; Mohn, F.; Moll, N.; Liljeroth, P.; Meyer, G. The chemical structure of a molecule resolved by atomic force microscopy. *Science* **2009**, *325*, 1110−4.
(13) Moresco, F.; Meyer, G.; Rieder, K.-H.; Tang, H.; Gourdon, A.; Joachim, C. Recording Intramolecular Mechanics during the Manipulation of a Large Molecule. *Phys. Rev. Lett.* **2001**, *87*, No. 088302.
(14) Ternes, M.; Lutz, C. P.; Hirjibehedin, C. F.; Giessibl, F. J.; Heinrich, A. J. The force needed to move an atom on a surface. *Science* **2008**, *319*, 1066−9.
(15) Pawlak, R.; Kawai, S.; Meier, T.; Glatzel, T.; Baratoff, A.; Meyer, E. Single-molecule manipulation experiments to explore friction and adhesion. *J. Phys. D: Appl. Phys.* **2017**, *50*, 113003.
(16) Kawai, S.; Koch, M.; Gnecco, E.; Sadeghi, A.; Pawlak, R.; Glatzel, T.; Schwarz, J.; Goedecker, S.; Hecht, S.; Baratoff, A.; Grill, L.; Meyer, E. Quantifying the atomic-level mechanics of single long physisorbed molecular chains. *Proc. Natl. Acad. Sci. U. S. A.* **2014**, *111*, 3968−3972.
(17) Kawai, S.; Benassi, A.; Gnecco, E.; Söde, H.; Pawlak, R.; Feng, X.; Müllen, K.; Passerone, D.; Pignedoli, C. A.; Ruffieux, P.; Fasel, R.; Meyer, E. Superlubricity of graphene nanoribbons on gold surfaces. *Science* **2016**, *351*, 957−961.
(18) Pawlak, R.; Vilhena, J. G.; Hinaut, A.; Meier, T.; Glatzel, T.; Baratoff, A.; Gnecco, E.; Pérez, R.; Meyer, E. Conformations and cryo-force spectroscopy of spray-deposited single-strand DNA on gold. *Nat. Commun.* **2019**, *10*, 685.
(19) Lafferentz, L.; Ample, F.; Yu, H.; Hecht, S.; Joachim, C.; Grill, L. Conductance of a Single Conjugated Polymer as a Continuous Function of Its Length. *Science* **2009**, *323*, 1193−1197.
(20) Wagner, C.; Fournier, N.; Tautz, F. S.; Temirov, R. Measurement of the Binding Energies of the Organic-Metal Perylene-Teracarboxylic-Dianhydride/Au(111) Bonds by Molecular Manipulation Using an Atomic Force Microscope. *Phys. Rev. Lett.* **2012**, *109*, 076102.

DOI: 10.1021/acs.nanolett.9b04418
Nano Lett. 2020, 20, 652−657

(21) Langewisch, G.; Falter, J.; Fuchs, H.; Schirmeisen, A. Forces during the controlled displacement of organic molecules. *Phys. Rev. Lett.* **2013**, *110*, 036101.
(22) Chong, M. C.; Afshar-Imani, N.; Scheurer, F.; Cardoso, C.; Ferretti, A.; Prezzi, D.; Schull, G. Bright Electroluminescence from Single Graphene Nanoribbon Junctions. *Nano Lett.* **2018**, *18*, 175−181.
(23) Vilhena, J. G.; Gnecco, E.; Pawlak, R.; Moreno-Herrero, F.; Meyer, E.; Pérez, R. Stick-Slip Motion of ssDNA over Graphene. *J. Phys. Chem. B* **2018**, *122*, 840−846.
(24) Li, Z.; Tkatchenko, A.; Franco, I. Modeling Nonreactive Molecule-Surface Systems on Experimentally Relevant Time and Length Scales: Dynamics and Conductance of Polyfluorene on Au(111). *J. Phys. Chem. Lett.* **2018**, *9*, 1140−1145.
(25) Gigli, L.; Kawai, S.; Guerra, R.; Manini, N.; Pawlak, R.; Feng, X.; Müllen, K.; Ruffieux, P.; Fasel, R.; Tosatti, E.; Meyer, E.; Vanossi, A. Detachment Dynamics of Graphene Nanoribbons on Gold. *ACS Nano* **2019**, *13*, 689−697.
(26) Gigli, L.; Vanossi, A.; Tosatti, E. Modeling nanoribbon peeling. *Nanoscale* **2019**, *11*, 17396−17400.
(27) Crawford, A. G.; Liu, Z.; Mkhalid, I. A. I.; Thibault, M.-H.; Schwarz, N.; Alcaraz, G.; Steffen, A.; Collings, J. C.; Batsanov, A. S.; Howard, J. A. K.; Marder, T. B. Synthesis of 2- and 2,7-functionalized pyrene derivatives: an application of selective C-H borylation. *Chem. - Eur. J.* **2012**, *18*, 5022−35.
(28) Kawano, S.-I.; Yang, C.; Ribas, M.; Baluschev, S.; Baumgarten, M.; Müllen, K. Blue-Emitting Poly(2,7-pyrenylene)s: Synthesis and Optical Properties. *Macromolecules* **2008**, *41*, 7933−7937.
(29) Ouyang, W.; Mandelli, D.; Urbakh, M.; Hod, O. Nanoserpents: Graphene Nanoribbon Motion on Two-Dimensional Hexagonal Materials. *Nano Lett.* **2018**, *18*, 6009−6016.
(30) Cacelli, I.; Prampolini, G. Parametrization and Validation of Intramolecular Force Fields Derived from DFT Calculations. *J. Chem. Theory Comput.* **2007**, *3*, 1803−1817.

NOTE ADDED AFTER ASAP PUBLICATION

This paper was published ASAP on December 6, 2019, with incorrect Supporting Information files for Movies 2 and 3. The corrected version was reposted on December 10, 2019.

DOI: 10.1021/acs.nanolett.9b04418
Nano Lett. 2020, 20, 652−657